Punching shear resistance of flat slabs with rectangular columns

Dênio R. C. OLIVEIRA
Lecturer
University of Pará
Belém, Brazil

Guilherme S. MELO
Lecturer
University of Brasília
Brasília, Brazil

Paul E. REGAN
Formerly Professor
University of Westminster
London, United Kingdom

Summary

Fifteen tests of high strength concrete (≅60 MPa) flat slabs with rectangular supports are reported. The rectangularity rate ranged from 1 to 5 and three different loads patterns were used. The results indicate that current CEB Model Code 90 previsions tend to overestimate punching resistance when the relation between the column long side and the slab effective depth increases. A Finite Element analysis shows the influences of the shape of a support and the pattern of loading on the distribution of shear. Factors are proposed to consider the overall flexural behaviour of the slabs while using the control perimeter and basic shear resistance of the MC90, and it is demonstrated that this approach provides strength estimates better than those of MC90, BS 8110 and ACI 318. Also is discussed the problem of the punching capacity of slabs almost failing in flexure.

Keywords: concrete flat slabs, punching resistance, rectangular columns.

1. Introduction

Reinforced concrete flat plate floors with rectangular columns spanning predominantly in two or one direction are common types of structural elements. Most codes of practice do not give enough or relevant guidance to designers who need to consider safety in relation to punching resistance of the slabs, specially when high strength concrete is applied.

The resulting shear around the supports or concentrated forces is considered uniformly distributed along of a recommended control perimeter by many codes and authors. This assumption is contrary what might reasonably be expected once considers the overall flexural behaviour of the slabs.

This article describes a series of fifteen tests and brings results from finite element analyses. Tests carried out by others authors were analysed and a simple modification of the approach to punching given in CEB Model Code 90 is presented. The method proposed is not a complete solution to all the problems, but its results were satisfactory when compared to most available test data.

2. Test program

Fifteen slabs with overall dimensions of 2280x1680x130 mm were tested. The main reinforcement was composed by fifteen 12.5 mm bars in the long direction with a nominal cover of 10mm and twenty-three 12.5 mm bars in the short direction, giving ratios of flexural reinforcement of 1.1% in both ways and a nominal mean effective depth of 107.5 mm. The ends of these bars were anchored with 6.3 mm hairpin bars. Reinforcement details are shown in Figure 1. Table 1 summarizes the main slab properties.

The supports were simulated by steel plates with 50 mm of thick, width of 120 mm and lengths varying from 120 to 600 mm (1.12 to 5.58·d), all located at the centre of the slabs. Equal loads were applied through steel beams close to the slab edges. In slabs type “a” and “b” the loads were at only two opposite short and long edges respectively while in type “c” all four edges were loaded. The test arrangements for a type “c” slab are shown in Figure 2. Four load cells were used.

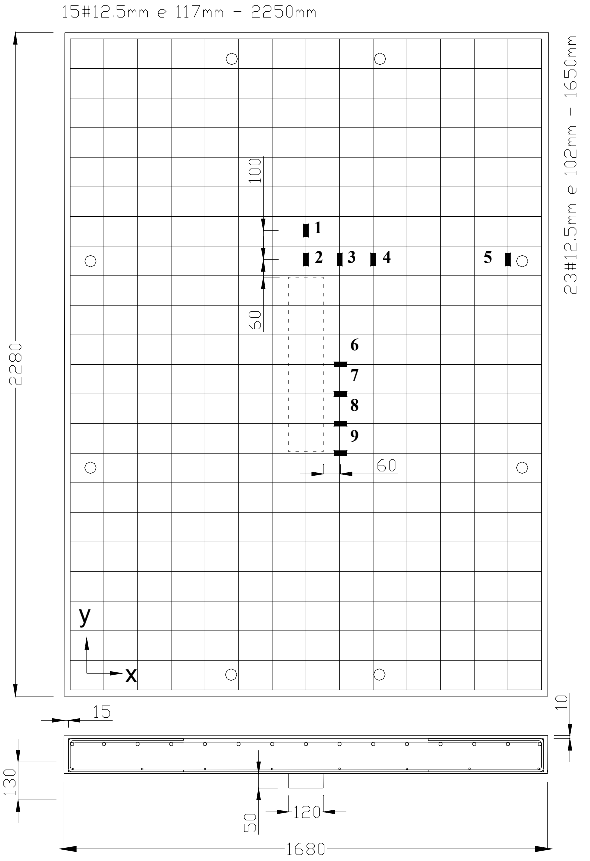

Fig. 1 Flexural reinforcement details and positions of strain gauges

Table 1 Characteristics of the tested slabs

Slab	d (mm)	ρ (%)	f_c' (MPa)	Column (mm) c_{min}	Column (mm) c_{max}	V_{Test} (kN)
L1a	107	1.09	57	120	120	240.0
L1b	108	1.08	59	120	120	322.4
L1c	107	1.09	59	120	120	318.0
L2a	109	1.07	58	120	240	246.0
L2b	106	1.10	58	120	240	361.0
L2c	107	1.09	57	120	240	330.8
L3a	108	1.08	56	120	360	240.6
L3b	107	1.09	60	120	360	400.0
L3c	106	1.10	54	120	360	357.6
L4a	108	1.08	56	120	480	250.8
L4b	106	1.10	54	120	480	395.0
L4c	107	1.09	56	120	480	404.0
L5a	108	1.08	57	120	600	287.4
L5b	108	1.08	67	120	600	426.4
L5c	109	1.07	63	120	600	446.4

Failure modes: Group "a" slabs: Flexural-punching
Groups "b" and "c" slabs: Punching

Materials, instrumentation and procedure

The concrete used throughout had the mix proportions given in Table 2. Cement CPII F32 is an Ordinary Portland Cement with a 6-10% content of filler which is primarily crushed limestone. Compression strengths were determined from tests of 100 x 200mm cylinders, cured and stored with the slabs.

The main reinforcement was of deformed bars with a yield stress of 749 MPa and an ultimate strength of 903 MPa. Stress-strain relationships from tests of the main reinforcement are given in Figure 3. Slab deflections were measured using dial gages mounted from independent frames and reading onto targets on the top surfaces of the slabs. Strains of reinforcement were measured at the positions shown in Figure 1 using pairs of gauges with 5 mm gauge lengths so that averaged values could eliminate local bending effects. Radial strains of the bottom surface of the concrete were measured also using electrical resistance gauges (gauge length 31.8 mm). Loads were applied in increments of 40 kN of total load and, after each, the slabs were inspected for cracking and measurements were taken.

3. Results

All of the tests ended in shear failures. The type "c" slabs, with loads at four sides, failed in a normal punching mode. The failure surfaces for slabs type "a" and "b" with small reaction areas were similar, but when $c_{max} \geq 360$ mm the failure surfaces in the type "a" slabs did not run around the longer sides of the reactions (see Figure 4).

As is confirmed by calculations of flexural capacities of the type "a" slabs were very close to flexural failure. In types "b" and "c" the failures were purely by punching. The deflection data showed that the displacements of the slabs along the lines at which measurements were made increased practically linearly with distance from the reaction area. The dial gauge readings from each line were used to calculate rotations and averaged to obtain transverse and longitudinal values. Figure 5 shows the greater averaged rotations plotted against total load for slabs L1a, L5a, L3b and L3c. The figure shows the difference in behaviour between types "a", "b" and "c" very clearly.

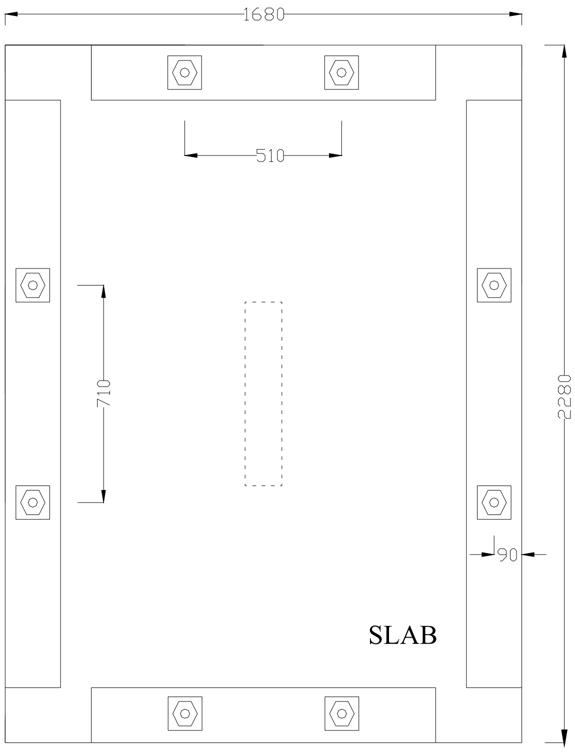

Fig. 2 Loading system (plan)

Table 2 Mix Proportions

Materials	kg / m^3
Cement (CP II – F32)	600
Silica Fume	60
Crushed Limestone (16 mm)	1092
Sand (5mm down)	512
Water	180
Superplasticizer	7.2

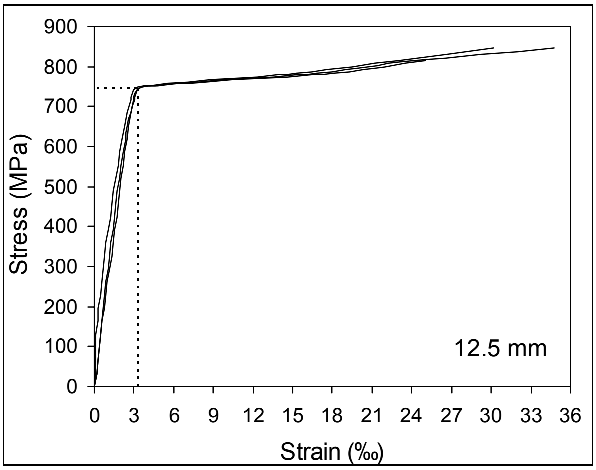

Fig. 3 Stress strain graphs for reinforcement

Inclination angles were measured considering the effective depth of the slabs and the average inclination for all failure surfaces (*x* and *y* direction) was approximately 25^o.

In type "a" slabs, the strains measured on the bars in the direction of the main span, 60 mm from the edge of the reaction zone, showed yielding of all bars within a width 2.2·d from the centre line. At the edge the strain reached 11.56‰ in slab L1a and 3.1 to 3.6‰ in the other slabs. None of the strains of the transverse bars exceeded 1.55‰. In the type "b" slabs, spanning predominantly in the shorter direction there was no yielding of the long (transverse) bars. The main bars did not yield in L1b, but yielding was recorded in others slabs, which were however very close to the loads.

A comparison between the experimental ultimate loads and the unfactored resistances according to ACI-318 [1], BS 8110 [2] and CEB-MC90 [3] is shown in Figure 6. For the type "a" slabs all three codes overestimate resistance and this is almost certainly because of the partly flexural nature of the failures. For the other two types ACI-318 is safe but not very consistent, while BS 8110 and MC90 resistances are close to the actual strengths for the smaller supports but tend to become unsafe for the larger ones.

Finite element analysis

All the slabs were modelled and analysed using the finite element method through the program Structural Analysis Program-SAP. The mesh was the same for all slabs and the applied loads were the failure loads. The elements used were rectangular shell with 60x60 mm and four joints. The aim of the analysis was to investigate the shear force distribution around the columns and along the Model Code control perimeter. This perimeter was adopted to plot the results due to both its reasonable concordance with the failure surfaces from the tests and its giving good results for the integration of the shear forces.

For slabs type "b" and "c" the nodes at the boundaries and within of the support areas were pinned. For slabs type "a" only the three nodes at the short sides were pinned since central upward displacements were observed in the tests. Loads were applied uniformly along lengths of 480 mm at short edges and/or 660 mm at long edges.

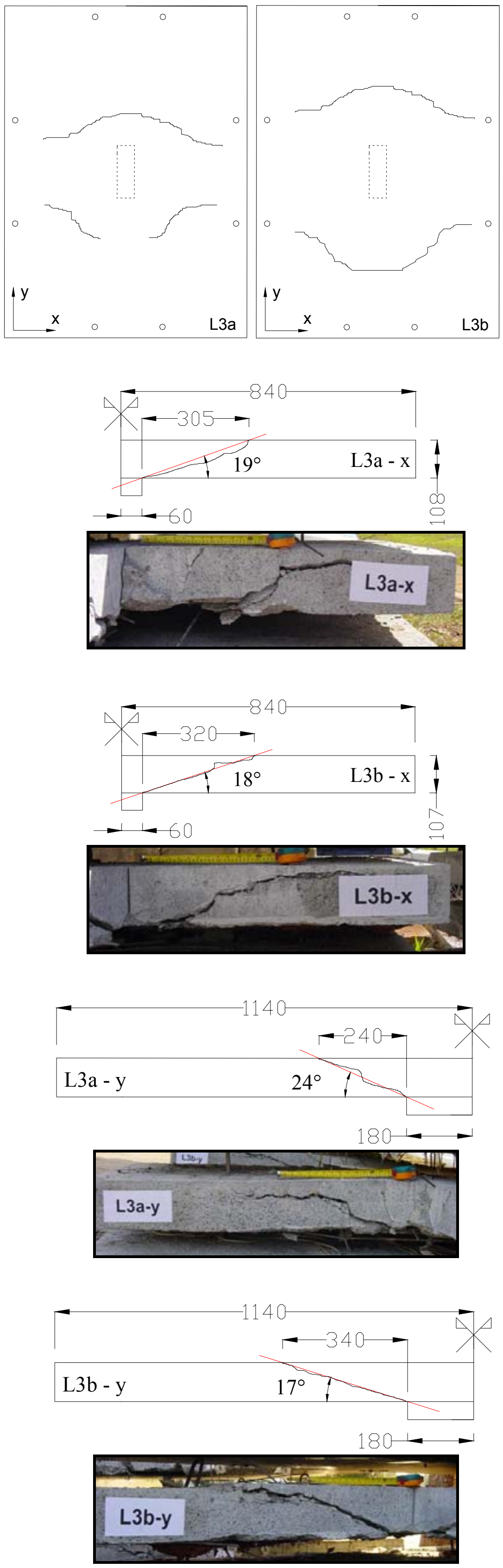

Fig. 4 Failure surfaces of the slabs L3a and L3b

An example of the shear force contours around the column is presented in Figure 7. For all slabs with $\frac{c_{max}}{c_{min}} > 1$ was possible to note clearly the influence of the column shape on the shear polarization even for one-way slabs where the applied load is parallel to the long side of the column. This characteristic is not present in the shear distributions along the Model Code control perimeter shown in Figure 8. At the Model Code perimeter, the shears are greatest near the support sides perpendicular to the spans for slabs of types “a” and “b” and the variation around the perimeter increases with the ratio c_{max}/c_{min}. For type “a” the ratio of the maximum to the average shear rises from 1.17 for c_{max}/c_{min}=1.0 to 1.64 for c_{max}/c_{min}=5. For type “b” the variation is much smaller and reaches only 1.23 for slab L5b. In type “c”, with half the loading applied at the short edges, this value was 1.60 for slab L5c.

If the maximum shears from Figure 8 are compared with the unfactored Model Code values from Equation 1 calculated for the parts of the perimeters where the shears are highest, the total average ratio v_{Elast}/v_{MC90} =1.13 can correct the predictions of MC90 and the average ratio v_{Exp}/v_{MC90} rises from 0.90 to 1.01 for types “b” and “c”. For type “a” the value 1.13 did not improve the predictions of MC90 giving an average ratio v_{Exp}/v_{MC90} =0.70 once there is the problem of the proximity of flexural failure.

$$v_{Rk} \cdot d = 0.18 \cdot \xi \cdot \sqrt[3]{100 \cdot \rho \cdot f_c'} \cdot d \qquad (1)$$

With $\xi = 1 + \sqrt{\frac{200}{d}}$

Is proposed here to take account of the effects of the shear polarization by factors to be incorporated in the Model Code for cases of symmetrical punching for two-way and one-way slabs.

For design an effective applied shear force ($V_{Sd,eff} = \lambda \cdot V_{Sd}$) should be calculated such that ($V_{Sd,eff}/(u_1 \cdot d)$) can be compared with the normal shear resistance $v_{Rd} = v_{Rk}/\gamma_m$. For comparison with test data the Equation 2 is proposed.

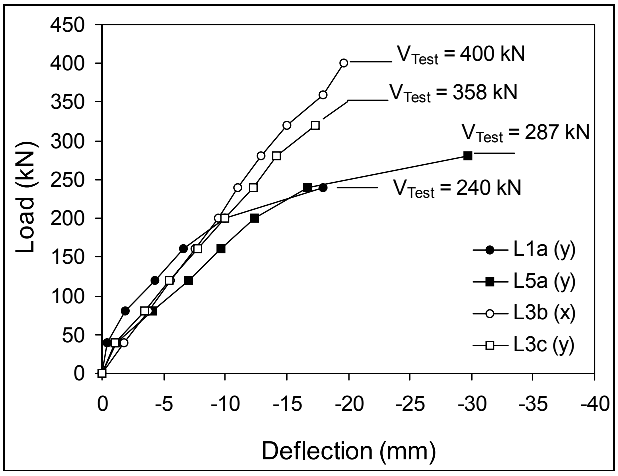

Fig. 5 Load v deflection

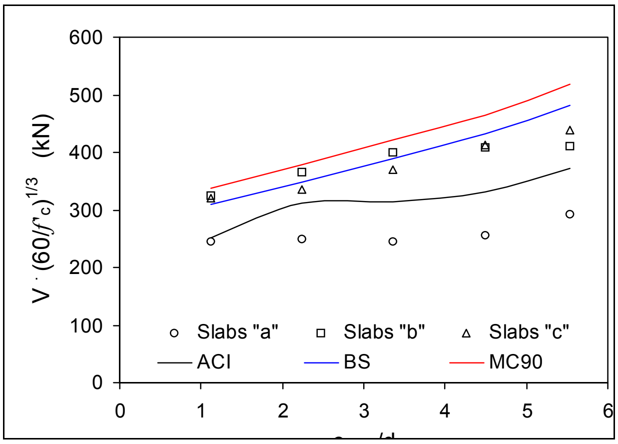

Fig. 6 Test and predicted results

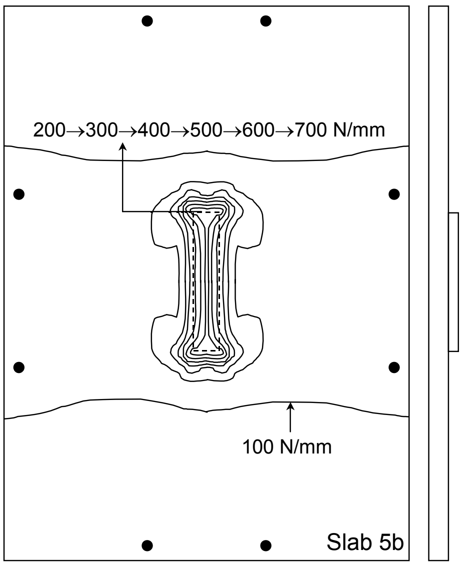

Fig. 7 Shear contours for slab L5b

Values for λ have been derived from available test data (85 slabs) taking account of the principal conditions which can occur relating to the directions in which a slab spans and the orientations of the longer and shorter sides of rectangular supports. The corresponding expressions for λ are given in Table 3.

The tests of Mowrer and Vanderbilt (1956)[4] are useful as they include slabs loaded through large square columns, but they introduce the problem of lightweight aggregate concrete in association with a very small effective depth. To be able to use this data in considering the effect of column size the predictions of Equation 2 have been multiplied by 0.9 to give an average V_{Test} / V_{Prop} of 1.0.

$$V_{Prop} = \frac{0.18}{\lambda}\cdot\xi\cdot\sqrt[3]{100\cdot\rho\cdot f_c'}\cdot d\cdot u_1 \qquad (2)$$

For the other methods of calculating resistances considered here the lightweight aggregate factors of ACI-318 and BS 8110 have been taken into account, while no correction has been made for MC90 which does not treat lightweight concrete. The results obtained are given in Table 4 where it can be seen that the proposed approach reduces the coefficient of variation of V_{Test} / V_{Prop} relative to those of all three codes, excluding slabs "a".

The strengths of the present type "a" slabs are not predicted satisfactorily by using the λ factors above. The main reason for this is probably a lowering of resistance due to wide cracks and high concrete strains. In the case of these slabs there is probably an additional effect from an increasing concentration of shear to the column faces perpendicular to the span as transverse yield lines develop. In the extreme this could reduce the active part of the control perimeter to that obtained at two edge columns contacting a slab only at their inner faces as shown in Figure 9 for which the shear resistance (V_{Min}) could be estimated using Equation 1 with $u_1 = (2\cdot c + 3\cdot\pi\cdot d)$. Table 5 summarizes the results for the type "a" slabs. The data is too limited for any definite conclusion to be reached but it appears that the ultimate resistances of such slabs when very close to flexural failure might be calculated by either reducing the normal estimate of VMC90/λ by 30% or considering the reduced perimeter of Figure 9. An alternative approach would be to accept the reduction in the ratio λ·(VTest/VMC90) on the basis that the partial safety factor on resistance can be allowed to decline from 1.5 for a shear failure to 1.15 for a flexural failure (1.15/1.5=0.77).

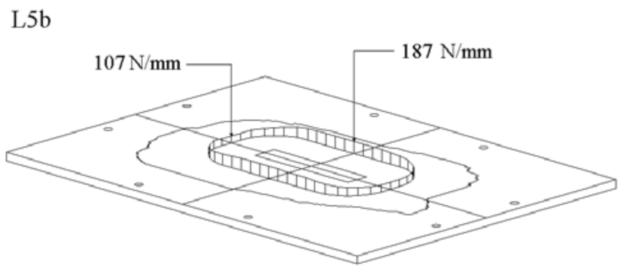

Fig. 8 Shear forces along the MC90 perimeter

Table 3 Flexural factors λ

Situation	λ
Two-way slabs (Type 1)	$1.03 \cdot (c_{max}/d)^{0.02}$
One-way (Type 2) $c_{max} \geq c_{min}$ parallel to span	$(c_{max}/d)^{0.17}$
One-way (Type 3) c_{max} perpendicular to span	$0.93 \cdot (c_{max}/d)^{0.14}$

Table 4 Comparison of results

Codes and Proposal	V_{Test}/V_{Calc}					
	Normal concrete			Light concrete		
	Av	Sd	Cv (%)	Av	Sd	Cv (%)
ACI	1.37	0.22	16.23	1.70	0.30	17.41
BS8110	1.01	0.09	8.53	1.18	0.09	7.89
CEB	0.95	0.09	9.04	0.84	0.06	7.49
Proposal	**1.00**	**0.06**	**5.77**	**1.00**	**0.06**	**6.21**

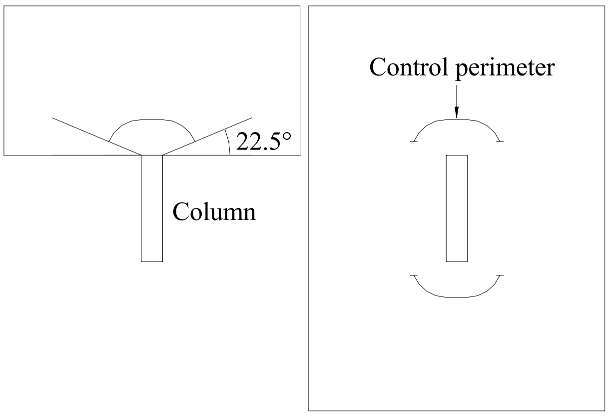

Fig. 9 Possible perimeter for type "a" slabs

Table 5 Results for slabs "a"

Slab	V_{Test} (kN)	$\frac{V_{Test}}{V_{Flex}}$	$\frac{\lambda \cdot V_{Test}}{V_{CEB}}$	$\frac{V_{Test}}{V_{Min}}$
L1a	240	1.00	0.74	1.06
L2a	246	0.94	0.73	1.06
L3a	241	0.88	0.70	1.06
L4a	251	0.85	0.69	1.11
L5a	287	0.91	0.75	1.26

4. Conclusion

The results of the tests reported here and others in the literature show that the punching resistances of flat slabs are influenced by the shapes and sizes of their supports and by their overall flexural behaviour in ways not properly accounted for in current code provisions. With the proposed values of □ included, the modified CEB-FIP method gives predictions of ultimate strengths which are significantly better than those of the unmodified Model Code, ACI-318 and BS 8110.

There remains the problem of the reduction of punching capacity, which occurs when the load is very close to a slab's flexural resistance. This is discussed, and two methods of obtaining approximate ultimate loads are given, although a partial safety factor reduction makes such calculations unnecessary.

References

1. ACI 318:2002. Building Code Requirements for Structural Concrete, American Concrete Institute, Farmington Hills, Michigan, 2002.

2. BS 8110:1997. Structural Use of Concrete, Part 1, Code of Practice for Design and Construction, British Standards Institution, London, 1997.

3. CEB-FIP. Model Code 1990, Thomas Telford, London, 1993.

4. MOWRER, R. D., VANDERBILT, M. D., Shear strength of lightweight aggregate reinforced concrete. ACI Journal, 1967, Vol. 64, No. 11, November, pp. 722-729.